

УДК 553.96:661.183

## Conversion of Alexandriya Brown Coal Into Microporous Carbons Under Alkali Activation

Yuliya V. Tamarkina\*, Tatyana G. Shendrik,  
Vladimir A. Kucherenko and Tatyana V. Khabarova

*L.M. Litvinenko Institute of Physical-Organic and Coal Chemistry,  
National Academy of Sciences of Ukraine,  
70 R. Luxemburg st., Donetsk, 83114 Ukraine*<sup>1</sup>

Received 2.03.2012, received in revised form 9.03.2012, accepted 16.03.2012

*We studied the pore structure of activated carbons (ACs) formed during the thermolysis of Aleksandriya brown coal (Ukraine), which was preliminary impregnated with alkali metal hydroxides, MOH with M being Li, Na, or K. We explored how pore structure parameters such as surface area, a total pore volume, meso- and micropore volume are modified with changing processing parameters such as temperature, an alkali/coal ratio (up to 2 g/g) and the nature of alkali cation. We also determined pore size distribution for meso- and micropores and compared all the three hydroxides as to their effect on porosity development. The formation of microporous structure is evidenced on heating a KOH-impregnated coal (1 g/g) from 400 to 800 °C: a surface area rises from 13 to 1005 m<sup>2</sup>/g, while a micropore volume fraction increases from 1 to 68 % of the total pore volume. Microporous carbon is formed at 800 °C over 1 h in a yield of 30 % with  $S_{\text{BET}}=1005$  m<sup>2</sup>/g, a total pore volume of 0.55 cc/g and a micropore volume of 0.38 cc/g. The total pore volume grows monotonously in the range LiOH<NaOH<KOH. Potassium hydroxide is found to promote microporosity development, whereas both LiOH and NaOH (at 18 mmol/g) act as inhibitors for micropore growth.*

*Keywords: brown coal, alkali activation, microporosity.*

### Introduction

Various raw materials, especially coals of different rank, are able to be transformed into activated carbons (ACs) by chemical activation with alkali hydroxides, MOH (M=Li, Na, K) [1]. At the present time, the studies of alkali activation focus on high rank coals, especially anthracites [2-9]. Anthracites may be converted into ACs with highly developed surface area ( $S_{\text{BET}}=2000-3000$  m<sup>2</sup>/g), but this requires a great amount of alkali to be used (up to 7g per gram of coal [9]).

\* Corresponding author E-mail address: [y\\_tamarkina@rambler.ru](mailto:y_tamarkina@rambler.ru)

<sup>1</sup> © Siberian Federal University. All rights reserved

Earlier, extensive studies were conducted for brown coals, which display a higher reactivity toward alkalis [10-13]. Alkali activation of brown coal results in AC with a surface area about 1000 m<sup>2</sup>/g under a relatively moderate alkali/coal ratio (~1 g/g). Brown coals contain a great amount of oxygenated functionalities reacting with MOH at room temperature for both traditional techniques of MOH-coal mixture preparation, i.e. impregnation and simple mixing. Such reactions involve interactions between alkalis and OH-acidic groups (phenolic and carboxylic) [14], heterolysis of C-O bonds in esters with phenolates and carboxylates as products [15], and the generation of semiquinone anion radicals [16]. The reactions proceed along with the diffusion of M<sup>+</sup>, OH<sup>-</sup> and MOH species into coal, helping the fixation of M<sup>+</sup> and OH<sup>-</sup> anions in the neighboring electron-donor and electron-acceptor sites within the carbon framework, and also favoring the formation of alkali humates. The products of such interactions (particularly humates) enable stronger binding action [10-12], allowing starting materials to be used as pelletized, extruded or other molds for chemical activation with no additional binder. A similar molding ability can be developed for higher-rank coals (e.g., bituminous ones [17]), but this requires preliminary coal oxidation to be conducted for building up oxygenated functionalities, which provides better coal reactivity toward MOH.

There are large deposits of brown coal in Ukraine (6-8·10<sup>9</sup> tons according to the Ukrainian ministry of coal industry). The most important deposit is found in Aleksandriya (Kyrovograd region), with its capacity being evaluated to be 0.5·10<sup>9</sup> tons, making it an important natural resource for producing activated carbons. Aleksandriya brown coal possesses all the above properties of brown coals. Besides, this coal is known to have a great content of montan wax (up to ~8 %). The last contains long-chain (C<sub>24</sub>-C<sub>30</sub>) carboxylic acid esters (~60 wt %) and free long-chain organic acids (~13 wt %) [18]. When impregnated or mixed with alkali, waxes are able to form fatty acid salts and *high molecular weight alcohols distributed within the coal framework*. Thus, such transformations may affect the properties of activated carbons.

This study is generally devoted to the investigation of Aleksandriya brown coal alkali activation and the properties of derived microporous carbons. We believe this to be a new point since chemical activation of this coal has not been studied and the quality of resulting activated carbons is not clear.

At the present point in time, our work focuses on exploring the effect of activation parameters (temperature, the type and content of alkali) on the properties of carbons from alkali activated brown coal, with particular attention paid to their pore structure.

## 1. Experimental

### 1.1. Brown coal

A brown coal of 500 kg selected from the Aleksandriya deposit (Kyrovograd region, Ukraine) was averaged, ground, sieved, and air-dried. All the experiments were conducted using particles of 0.5-1.0 mm in size. Coal is characterized as follows (%): W<sup>a</sup> 12,4; A<sup>d</sup> 11,7; V<sup>daf</sup> 57,6; C<sup>daf</sup> 70,4; H<sup>daf</sup> 6,0; S<sup>daf</sup> 3,8; N<sup>daf</sup> 2,0; O<sup>daf</sup><sub>diff</sub> 17,8.

### 1.2. Coal impregnation

Brown coal was preliminarily dried at 105 °C for 2 h. A 100 g coal sample was mixed with a 30% aqueous alkali solution. The mixture was held for 24 h at room temperature and dried at 120 °C until

constant weight. The alkali solution was taken in an amount providing the required MOH/coal ratio ( $R_{\text{MOH}}$ ), expressed as grams or moles of MOH per g of dry coal. In a blank experiment, a coal sample was soaked with the same quantity of water as that of alkali solution, then held for 24 h and finally dried under the same conditions as the KOH-treated samples.

### 1.3. Heat treatment

The solid products (SP) of thermolysis were produced by heating the original or alkali impregnated coal samples in a vertical furnace of 0.2 dm<sup>3</sup>.

The samples were heat-treated under a 2 dm<sup>3</sup>/h argon flow as follows: 1) temperature-programmed heating with a rate of 4°C/min up to a temperature selected between 400 °C and 800°C; 2) holding the sample at a given temperature for 1 hour; 3) cooling down to room temperature. The heat-treated samples were washed off with distilled water, then with 0.1 M HCl, and once again with water until the negative response of Cl<sup>-</sup> ions against AgNO<sub>3</sub>. The washed samples were dried at 105±5°C.

The solid products derived from brown coal thermolysis are referred to as SP. The products produced using LiOH, NaOH, KOH are denoted as AC-Li, AC-Na and AC-K, respectively.

### 1.4. Characterization of pore structure

Pore structure was explored by the analysis of N<sub>2</sub> adsorption/desorption isotherms for the samples outgassed at 200 °C for 20 h. The isotherms were recorded at 77 K using a Quantachrome Autosorb 6B instrument. The specific surface area  $S_{\text{BET}}$  (m<sup>2</sup>/g) was determined from the BET analysis of the isotherm portion corresponding to a relative N<sub>2</sub> pressure  $p/p_o$  below 0.3 [19]. The total pore volume  $V_{\Sigma}$  (cm<sup>3</sup>/g) was determined using the amount of nitrogen adsorbed at  $p/p_o \sim 1$ .

Mesopore size distribution and the volume of mesopores –  $V_{\text{me}}$  (cm<sup>3</sup>/g) were evaluated by the BJH method [20] using the desorption branch of N<sub>2</sub> gas isotherms. The mesopore volume  $V_{\text{me}}$  was determined from the cumulative volume curves by accounting only for the volume of pores 2-50 nm in diameter.

The micropore volume  $V_{\text{mi}}$  (cm<sup>3</sup>/g) was determined using the Dubinin-Radushkevich method [21]. Micropore size distribution was evaluated using the DFT method [22]. The surface area  $S_{\text{DFT}}$  and the volume of subnanopores  $V_{1\text{nm}}$  (pores less than 1 nm) were assessed from the DFT cumulative curves for the specific surface and volume, correspondingly.

## 2. Results and discussion

### 2.1. Pore structure as function of temperature

It was established earlier that the optimum parameters for developing the pore structure of activated carbons includes isothermal exposure for 1 h at a KOH/coal ratio,  $R_{\text{KOH}}=1$  g/g [23]. With these parameters maintained, we studied the changes in AC properties as a function of processing temperature [24].

**Yield.** The yield of solid products decreases as temperature rises (Fig. 1), amounting to 44.4% for SP and 31% for AC-K at 800 °C. The lower yield in AC-K in comparison to SP is connected with a greater amount of volatile gaseous products produced as a result of the alkali destruction of C-C and C-O bonds in the carbon framework, including those bonds related with cyclic esters and heterocycles [15].

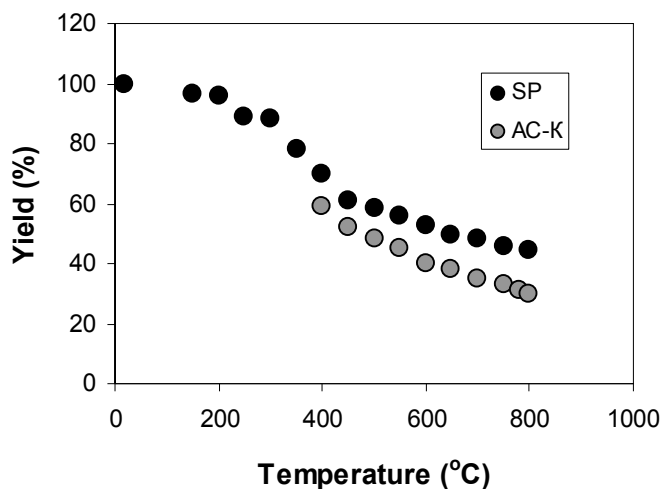


Fig. 1. Changes in the SP and AC-K yield

**Changes in specific surface area** for SP and AC-K products with increasing temperature are given in Table 1. At temperatures below 400°C, the specific surface area of parent coal equals  $S_{\text{BET}} = 8\text{--}9 \text{ m}^2/\text{g}$  (as measured after drying at 120°C), whereas the SP products are formed with a lower specific surface area (5  $\text{m}^2/\text{g}$ ). On the contrary, the AC-K products (KOH thermolysis) display an insignificant increase in  $S_{\text{BET}}$ , up to 13  $\text{m}^2/\text{g}$ . Between 400 °C and 500 °C,  $S_{\text{BET}}$  goes up abruptly and then increases continuously up to  $S_{\text{BET}}=1005 \text{ m}^2/\text{g}$  at 800°C if KOH is present. By contrast, for the SP samples (prepared without potassium hydroxide), heating up to 600°C does not significantly alter the specific surface area ( $S_{\text{BET}}=15 \text{ m}^2/\text{g}$ ); further increasing temperature leads to a maximum of  $S_{\text{BET}} = 272 \text{ m}^2/\text{g}$  at 700°C, with a little shift in  $S_{\text{BET}}$  down to 235  $\text{m}^2/\text{g}$  at 800°C.

**Total pore volume ( $V_{\Sigma}$ )** does not change greatly up to 400°C for samples AC-K, but rises sharply if temperature is further increased up to 800 °C (Table 1). For temperatures between 400 and 800 °C,  $V_{\Sigma}$  depends almost linearly on  $t$  and can be approximated as  $V_{\Sigma}=0.0011t-0.3271$  ( $R^2=0.951$ ). For temperatures between 400 °C and 500°C, no abrupt change is observed for the  $V_{\Sigma}$  values, as distinct from the  $S_{\text{BET}}$  values of AC-K.

KOH-free coal thermolysis does not induce a significant change in the pore volume up to temperatures of about 600°C, with  $V_{\Sigma}=0.05\text{--}0.08 \text{ cm}^3/\text{g}$ . Further increasing temperature involves a larger pore volume of solid products, with their maximum values,  $V_{\Sigma}=0.17\text{--}0.20 \text{ cm}^3/\text{g}$  for 750–800°C.

Potassium hydroxide promotes porosity development, with  $V_{\Sigma}$  values increasing for samples AC-K over the whole temperature range. Between 400 and 600°C, alkali generates pores extensively, whereas this is not the case if no KOH is used. Strong porosity development is observable between 600–800°C for either SP or AC-K. However, in the presence of alkali, pore formation proceeds with more intensity, resulting in the products whose total pore volume is 3 times larger.

**Mesoporosity.** Mesoporosity is developed much better if KOH is present (Table 1). For AC-K products, a mesopore volume is progressively developed with maximum values being reached at 700°C ( $V_{\text{me}}=0,19\pm 0,01 \text{ cm}^3/\text{g}$ ). Higher temperature involves a  $V_{\text{me}}$  decay, although the total pore volume in fact increases (Table 1). A mesopore fraction,  $V_{\text{me}}/V_{\Sigma}$  (Table 1), goes down from 0.58 to 0.22.

Table 1. Porosity characterization for samples SP and AC-K, produced at different temperatures

| t, °C | Sample            | $S_{\text{BET}}$ ,<br>$\text{m}^2/\text{g}$ | $V_{\Sigma}$ ,<br>$\text{cm}^3/\text{g}$ | $V_{\text{mi}}$ ,<br>$\text{cm}^3/\text{g}$ | $V_{\text{mi}}/$<br>$V_{\Sigma}$ | $V_{\text{me}}$ ,<br>$\text{cm}^3/\text{g}$ | $V_{\text{me}}/$<br>$V_{\Sigma}$ |
|-------|-------------------|---|--|---|----------------------------------|---|----------------------------------|
| 120   | SP                | 8   | 0.048                                    | 0.003                                       | 0.06                             | 0.028                                       | 0.58                             |
|       | AC-K <sup>1</sup> |   |  |   |                                  |   |                                  |
| 400   | SP                | 5   | 0.082                                    | 0.001                                       | 0.01                             | 0.022                                       | 0.27                             |
|       | AC-K              | 13  | 0.095                                    | 0.001                                       | 0.01                             | 0.052                                       | 0.55                             |
| 500   | SP                | 8   | 0.070                                    | 0.003                                       | 0.05                             | 0.018                                       | 0.26                             |
|       | AC-K              | 273   | 0.281                                    | 0.079                                       | 0.28                             | 0.123                                       | 0.44                             |
| 550   | SP                | 11  | 0.052                                    | 0.004                                       | 0.07                             | 0.021                                       | 0.40                             |
|       | AC-K              | 370   | 0.262                                    | 0.139                                       | 0.53                             | 0.096                                       | 0.37                             |
| 600   | SP                | 15  | 0.077                                    | 0.005                                       | 0.06                             | 0.019                                       | 0.25                             |
|       | AC-K              | 450   | 0.384                                    | 0.167                                       | 0.43                             | 0.162                                       | 0.42                             |
| 650   | SP                | 163   | 0.100                                    | 0.020                                       | 0.20                             | 0.022                                       | 0.22                             |
|       | AC-K              | 555   | 0.392                                    | 0.210                                       | 0.54                             | 0.144                                       | 0.37                             |
| 700   | SP                | 272   | 0.152                                    | 0.068                                       | 0.44                             | 0.030                                       | 0.20                             |
|       | AC-K              | 695   | 0.496                                    | 0.265                                       | 0.53                             | 0.186                                       | 0.38                             |
| 750   | SP                | 253   | 0.199                                    | 0.089                                       | 0.45                             | 0.054                                       | 0.27                             |
|       | AC-K              | 773   | 0.476                                    | 0.294                                       | 0.62                             | 0.152                                       | 0.32                             |
| 800   | SP                | 235   | 0.172                                    | 0.111                                       | 0.65                             | 0.038                                       | 0.22                             |
|       | AC-K              | 1005  | 0.551                                    | 0.377                                       | 0.68                             | 0.127                                       | 0.23                             |

N.B. AC-K prepared at 120°C is not characterized as we were unable to remove KOH due to an intensive formation of potassium humates.

The SP materials show poorly developed mesoporosity. The mesopore volume of SP has low values, comprised within  $V_{\text{me}} = 0.02\text{-}0.03 \text{ cm}^3/\text{g}$ , and only does the SP material prepared at 750-800°C show a sensible increase in the mesopore volume with  $V_{\text{me}} = 0.04\text{-}0.05 \text{ cm}^3/\text{g}$ . A mesopore fraction also decreases for the SP samples (Table 1), equaling that of the KOH-made AC-K material at 800°C.

There are virtually no micropores for the SP-K products produced in the presence of KOH at  $t \leq 400^\circ\text{C}$ , and the SP samples do not show microporosity development up to 600°C. These products have a micropore volume less than  $0.005 \text{ cm}^3/\text{g}$ . In other words, their porosity is almost exclusively made up of mesopores and macropores.

**Microporosity** undergoes strong formation in the presence of alkali between 400°C and 800°C (Table 1). Particularly, there is a specific temperature range (400°C to 600°C) associated with micropore formation in the KOH treatment case only. The SP products (no KOH involved) do not possess micropores at the same temperatures, suggesting that micropores are developed solely owing to interactions between KOH and the organic coal matter.

At higher temperatures, between 600 and 800°C, the micropores are developed without KOH, most likely due to a deeper thermal destruction and some secondary reactions of gaseous coal products with a carbon-coated solid residue. A maximum micropore volume is seen for the products prepared at

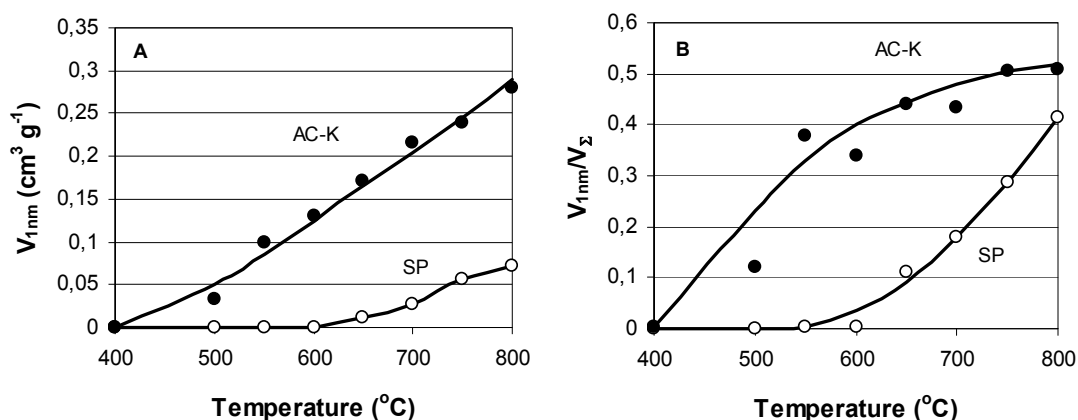


Fig. 2. Temperature dependence for the volume (A) and the fraction (B) of subnanopores for samples SP and AC-K

800 $^{\circ}\text{C}$ :  $V_{mi} = 0.38 \text{ cm}^3/\text{g}$  for AC-K and  $0.11 \text{ cm}^3/\text{g}$  for SP. In the presence of alkali, the micropore volume is 4 times larger, whereas the micropore fractions are close in values.

**Subnanopores.** We additionally determined the volume ( $V_{1nm}$ ) of pores less than 1 nm and its fraction (defined as  $V_{1nm}/V_{\Sigma}$ ) as a function of temperature. We draw particular attention to subnanopores since they are of utmost importance to both high hydrogen adsorption capacity [25] and high electrochemical capacitance [26].

The subnanopore volume  $V_{1nm}$  of activated carbons is greatly dependent on the activation conditions (Fig. 2, A). For temperature below 400 $^{\circ}\text{C}$ , materials SP and AC-K do not contain subnanopores ( $V_{1nm} = 0$ ). When alkali is used,  $V_{1nm}$  rises from  $2 \cdot 10^{-4} \text{ cm}^3/\text{g}$  at 400 $^{\circ}\text{C}$  to a maximum value of  $0.28 \text{ cm}^3/\text{g}$  at 800 $^{\circ}\text{C}$ , which makes up 51% of the total pore volume or 74 % of the micropore volume (Fig. 2, B). For the SP materials produced without KOH, such pores are formed if activation is conducted at temperature above 600 $^{\circ}\text{C}$  with  $V_{1nm} = 0.07 \text{ cm}^3/\text{g}$  at 800 $^{\circ}\text{C}$ .

The products formed at 800  $^{\circ}\text{C}$  have the most developed porosity. Therefore, a temperature of 800  $^{\circ}\text{C}$  was selected to probe nanoporosity development as a function of both the KOH/coal ratio and the nature of cation.

## 2.2. Effect of KOH/coal ratio

The effect of KOH/coal ratio is studied for the samples prepared at varied  $R_{\text{KOH}}$  (up to 2 g/g), all other parameters being held constant: a temperature of 800  $^{\circ}\text{C}$ , a heating rate of 4  $^{\circ}\text{C}/\text{min}$ , isothermal exposure at 800  $^{\circ}\text{C}$  for 1 h.

An AC-K yield exhibits an initial increase with increasing  $R_{\text{KOH}}$ , which is obvious at low KOH/coal ratios ( $R_{\text{KOH}} \leq 0.15 \text{ g/g}$ ) (Fig. 3). After reaching a maximum, a linear decrease in the AC-K yield is observed with growing  $R_{\text{KOH}}$ .

$S_{\text{BET}}$  is decreasing on increasing  $R_{\text{KOH}}$  up to  $R_{\text{KOH}} = 0.05\text{-}0.20 \text{ g/g}$ , with an  $S_{\text{BET}}$  minimum being reached at  $R_{\text{KOH}} = 0.05\text{-}0.20 \text{ g/g}$ . An inverse relationship is observed between  $R_{\text{KOH}}$  and  $S_{\text{BET}}$  for the higher  $R_{\text{KOH}}$  values (up to 0.8-1.0 g/g) (Fig. 3). Further increasing the alkali/coal ratio ( $R_{\text{KOH}} = 1\text{-}2 \text{ g/g}$ ) does not change the  $S_{\text{BET}}$  value, which equals 980-1030  $\text{m}^2/\text{g}$  within experimental error.

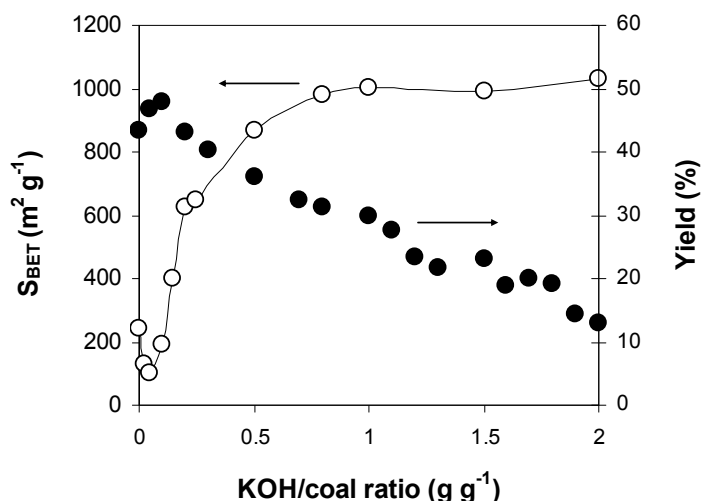


Fig. 3. The yield and specific surface area as a function of the KOH/coal ratio

A similar effect was observed earlier on the chemical activation of the same coal with sodium and lithium hydroxides [23]. At low  $R_{\text{MOH}}$  values,  $S_{\text{BET}}$  goes down on increasing an alkali/coal ratio, but to a varied extent for different alkalis. Porosity development is enhanced in the range  $\text{LiOH} < \text{NaOH} < \text{KOH}$ . A yield of solid products decreases following the same alkali range.

At low  $R_{\text{KOH}}$ , the increasing yield and the decreasing specific surface area both provide evidence for the predominance of condensation processes, which are likely to be promoted by  $\text{K}^+$  ions or potassium metal, the latter being created due to a thermally initiated reduction of  $\text{K}^+$  ions by the electrons of the carbon framework [3, 7-9, 27]. Such condensation reactions were established on the heat-treatment of coal with NaOH [28] and polyarenes with KOH (e.g., the condensation of benzanthrone into violanthrone above  $200^\circ\text{C}$  [29]), giving rise to the formation of additional cross-links and, finally, a more rigid spatial framework. This resulted in a yield increase of the solid product (Fig. 1), which is low-porosity carbon material, according to the values of  $S_{\text{BET}}$ ,  $V_{\Sigma}$ ,  $V_{\text{mi}}$ ,  $V_{\text{mi}}/V_{\Sigma}$  and  $S_{\text{mi}}/S_{\text{BET}}$ .

Both further increase in specific surface area and decrease in yield are associated with the preponderance of alkali destruction reactions. These involve the heterolysis of C-O- and polarized C-C- bonds, the cleavage of O- and S-containing heterocycles [15], the dehydration of arene and alkane fragments of the carbon framework [3, 27]. All these interactions bring about low molecular weight products (such as  $\text{H}_2$ ,  $\text{CH}_4$ , etc.). These reactions also decrease the yield of solid products, but they enable porosity growth, as evidenced by a substantial rise in the pore volume and specific surface area.

No change in the specific surface area and the fall in the AC-K yield for  $R_{\text{KOH}}=1.0-2.0$  g/g suggest that the preparation of activated carbons from the studied brown coal cannot be recommended at  $R_{\text{KOH}} > 1.0$  g/g.

Fig. 4 shows the pore size distribution determined using the BJH method [20] for SP and AC-K. Potassium hydroxide favors an intensive growth of pores about 4 nm in diameter, with their differential volume (denoted as  $dV_{4\text{nm}}/dD$ ) exhibiting a complicated dependence on the KOH/coal ratio (Table 2).

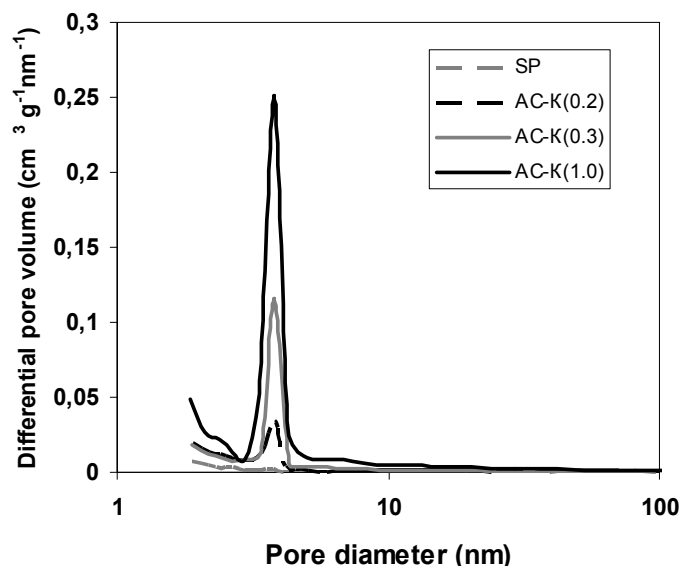


Fig. 4. Mesopore size distribution (the BJH method)

Table 2. Porosity characterization for samples SP and AC-K, produced at different coal/KOH ratios

| $R_{\text{KOH}}$ , g/g | $S_{\text{BET}}$ , $\text{m}^2/\text{g}$ | $V_{\Sigma}$ , $\text{cm}^3/\text{g}$ | $V_{\text{mi}}$ , $\text{cm}^3/\text{g}$ | $V_{\text{mi}}/V_{\Sigma}$ | $V_{\text{me}}$ , $\text{cm}^3/\text{g}$ | $V_{\text{me}}/V_{\Sigma}$ | $dV_{4\text{nm}}/dD$ , $\text{cm}^3/\text{g}$ |
|------------------------|--|---------------------------------------|--|----------------------------|--|----------------------------|---|
| 0                      | 235                                      | 0.172                                 | 0.111                                    | 0.65                       | 0.038                                    | 0.22                       | 0.010   |
| 0.05                   | 101                                      | 0.061                                 | 0.037                                    | 0.61                       | 0.006                                    | 0.1                        | <0.001  |
| 0.1                    | 190                                      | 0.104                                 | 0.061                                    | 0.59                       | 0.011                                    | 0.11                       | 0.002   |
| 0.2                    | 626                                      | 0.322                                 | 0.230                                    | 0.71                       | 0.058                                    | 0.18                       | 0.034   |
| 0.3                    | 707                                      | 0.376                                 | 0.261                                    | 0.69                       | 0.104                                    | 0.28                       | 0.116   |
| 0.6                    | 928                                      | 0.515                                 | 0.345                                    | 0.67                       | 0.174                                    | 0.34                       | 0.206   |
| 1.0                    | 1005                                     | 0.551                                 | 0.377                                    | 0.68                       | 0.127                                    | 0.23                       | 0.251   |

At  $R_{\text{KOH}} \rightarrow 0.1$  g/g, the value of  $dV_{4\text{nm}}/dD$  goes first down and then up. The value of  $V_{4\text{nm}}/V_{\Sigma}$  is low for samples with  $V_{\Sigma} \leq 0.1$   $\text{cm}^3/\text{g}$ ; this value increases as porosity is more developed.

The effect of KOH on the micropore size distribution of solid products can be followed from the comparison between curves 4 (AC-K) and 1 (SP) at the figure below where the DFT pore size distribution is discussed.

### 2.3. Effect of the nature of cation

The effect of the nature of cation was assessed for the samples prepared under the same processing conditions (4 °C/min, 800 °C, 1 h) at an equal molar MOH/coal ratio. The equal molar alkali/coal ratios were adopted for the following reason. We suppose that the development of the pore structure is caused by the same reactions with different alkali metal hydroxides. In case different alkalis result in different porosities, this is caused by the nature of the cation. For KOH, an optimum ratio was 1 g/g, *i.e.* 18 mmol



Table 3. Porosity parameters for the samples prepared using different alkalis (800 °C, 4 °C/min, 1h,  $R_{\text{MOH}}=18$  mmol/g)

|       | $S_{\text{BET}}$ ,<br>$\text{m}^2/\text{g}$ | $V_{\Sigma}$ ,<br>$\text{m}^3/\text{g}$ | $V_{\text{mi}}$ ,<br>$\text{cm}^3/\text{g}$ | $V_{\text{mi}}/$<br>$V_{\Sigma}$ | $V_{\text{me}}$ ,<br>$\text{cm}^3/\text{g}$ | $V_{\text{me}}/$<br>$V_{\Sigma}$ | $V_{1\text{nm}}$ ,<br>$\text{cm}^3/\text{g}$ | $V_{1\text{nm}}/$<br>$V_{\Sigma}$ | $dV_{4\text{nm}}/$<br>$dD$ |
|-------|---|---|---|----------------------------------|---|----------------------------------|--|-----------------------------------|----------------------------|
| SP    | 235   | 0.172                                   | 0.111                                       | 0.65                             | 0.038                                       | 0.22                             | 0.069  | 0.40                              | 0.009                      |
| AC-Li | 273   | 0.270                                   | 0.096                                       | 0.36                             | 0.132                                       | 0.49                             | 0.052  | 0.19                              | 0.112                      |
| AC-Na | 173   | 0.350                                   | 0.062                                       | 0.18                             | 0.199                                       | 0.57                             | 0.020  | 0.06                              | 0.142                      |
| AC-K  | 1005  | 0.551                                   | 0.377                                       | 0.68                             | 0.127                                       | 0.23                             | 0.280  | 0.45                              | 0.251                      |

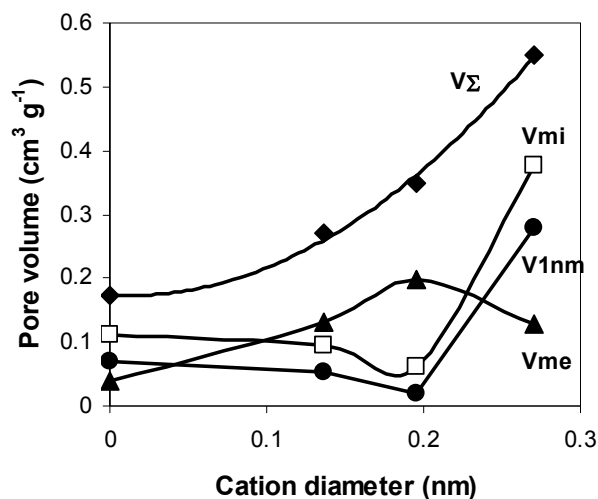


Fig. 5. Pore structure parameters of SP, AC-Li, AC-Na, AC-K vs alkali cation diameter

of KOH per 1 gram of coal. The same molar ratio was adopted when LiOH and NaOH were used. Porosity parameters for the samples of activated carbons are summarized in Table 3.

In comparison to the SP material (*i.e.* prepared without alkali), the surface of alkali activated carbons rises slowly with LiOH as an activating agent and much more significantly if KOH is used. Sodium hydroxide taken in an amount of 18 mmol/g suppresses surface area development (Table 3).

A rise in the total pore volume ( $V_{\Sigma}$ ) is observed as the alkali cation diameter increases ( $D_M$ ) (Table 3). The relation between  $V_{\Sigma}$  and  $D_M$  can satisfactorily be approximated as  $V_{\Sigma}=5,6 D_M^2 - 0,13 D_M + 0,174$  ( $R^2=0,996$ ). The micropore volume (pores at  $D \leq 2$  nm) experiences a 2-times decrease in the range SP – AC-Li – AC-Na, whereas it rises greatly on going to AC-K,  $V_{\Sigma} = 0.38$   $\text{cm}^3/\text{g}$  (Table 3). A similar trend is seen for the micropore fraction ( $V_{\text{mi}}/V_{\Sigma}$ ): the adsorbent derived from parent coal has the greatest  $V_{\text{mi}}/V_{\Sigma}$  value, close to that for AC-K. For AC-Na, the  $V_{\text{mi}}/V_{\Sigma}$  value is about 4 times lower.

The microporosity of SP from parent coal is formed due to the interaction between the carbon framework and the thermolysis gases only. KOH is an agent most efficiently contributing to micropore formation (Fig. 5). Microporosity development is suppressed when LiOH and NaOH are used (at least with an MOH/coal ratio of 18 mmol/g). This is surprising since NaOH is known to be an efficient

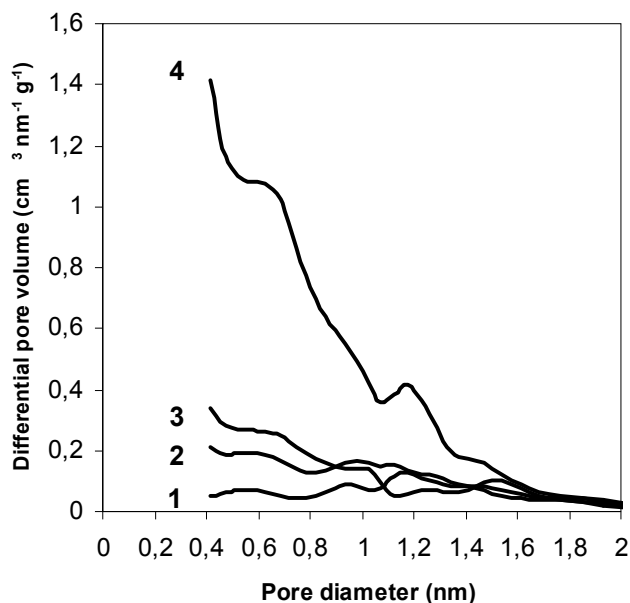


Fig. 6. DFT pore size distribution for AC-Na (1), AC-Li (2), SP (3), and AC-K (4)

activating agent [4, 6]. NaOH activation results in ACs with developed surface area, but at a large NaOH/coal ratio, usually 2-4 g/g. In our work, this ratio is essentially lower ( $R_{\text{NaOH}}=0.72$  g/g), and condensation processes may come about as those taking place under KOH activation at  $R_{\text{KOH}}\leq 0.1$  r/r (Fig. 3).

The micropore decrease in the range SP – AC-Li – AC-Na is compensated by mesopore increase in the same range (Fig. 5). As a result, monotonous increase of total pore volume is observed.

According to the differential distribution curves calculated using the BJH method, the adsorbent from parent coal exhibits approximately uniform pore size distribution (Fig. 4). Mesopore size distribution for AC-Li и AC-Na corresponds to that for AC-K. In the alkali-made samples, the fraction of pores with  $D\sim 4$  nm rises sharply. The effect is seen for all the studied alkalis, and is progressively stronger in the range AC-Li < AC-Na < AC-K (Table 3).

Micropore size distribution (pores with  $D\leq 2$  nm) is presented in Fig. 6. Lithium and sodium hydroxides do not induce the development of subnanopores, which is also noticeable from the dependence between  $V_{\text{1nm}}$  and cation diameter (Fig. 5). The differential pore volume within  $D=1-2$  nm has close values for SP, AC-Li и AC-Na. KOH develops micropores of all sizes and is the most efficient pore-forming agent. The values of total micropore volume calculated with the DFT method are (in  $\text{cm}^3/\text{g}$ ): 0.100 for SP; 0.092 (AC-Li); 0.051 (AC-Na); 0.365 (AC-K). These values are close to those determined using the Dubinin-Raduskevich method (Table 3).

### 3. Conclusions

1. Aleksandriya brown coal can be transformed into microporous carbon using heat-treatment with potassium hydroxide at 800 °C for 1 h. Derived microporous carbon has a specific surface area of  $\sim 1000$   $\text{m}^2/\text{g}$ , a total pore volume of  $\sim 0.55$   $\text{cm}^3/\text{g}$  and a micropore volume of  $\sim 0.38$   $\text{cm}^3/\text{g}$ .

2. The pore structure of KOH activated carbon is created at temperature 400-800°C. Increasing temperature induces an increase in  $S_{\text{BET}}$ , from 13 to 1005 m<sup>2</sup>/g, whereas  $V_{\Sigma}$  is increased from 0.095 cm<sup>3</sup>/g to 0.551 cm<sup>3</sup>/g, and  $V_{\text{mi}}$  from 0.001 cm<sup>3</sup>/g to 0.377 cm<sup>3</sup>/g.

3. Lithium and sodium hydroxides (at 18 mmol/g ratio) suppress the development of microporosity, which is compensated by the additional development of mesoporosity. As a result, the total pore volume grows monotonously in the range LiOH<NaOH<KOH.

4. Potassium hydroxide is the most efficient reagent for microporosity development in activated carbons made from Alexandriya brown coal.

### Acknowledgments

This work was supported by the National Academy of Sciences of Ukraine (under contract 0107U010881). We thank N.N. Tsyba from the Institute for Sorption and Problems of Endoecology, NAS of Ukraine, for cooperation in the N<sub>2</sub> adsorption study.

### References

1. H. Marsh, F. Rodriguez-Reinoso, Activated carbon, Amsterdam, Elsevier, 2006. 542 p.
2. Lozano-Castelló D., Lillo-Ródenas M.-A., Cazorla-Amorós D., Linares-Solano A. Preparation of activated carbons from Spanish anthracite: I. Activation by KOH // Carbon. 2001. V. 39. P. 741-749.
3. Yoshizawa N., Maruyama K., Yamada Y., Ishikawa E., Kobayashi M., Toda Y., et al. XRD evaluation of KOH activation process and influence of coal rank // Fuel. 2002. V. 81. P. 1717-1722.
4. Perrin A., Celzard A., Albinia A., Kaczmarczyk J., Marêché J.-F., Furdin G. NaOH activation of anthracites: effect of temperature on pore textures and methane storage ability // Carbon. 2004. V. 42. P. 2855-2866.
5. Pietrzak R., Jurewicz K., Nowicki P., Babel K., Wachowska H. Microporous activated carbons from ammoxidised anthracite and their capacitance behaviours // Fuel. 2007. V. 86. P. 1086-1092.
6. Celzard A., Perrin A., Albinia A., Broniek E., Marêché J.-F. The effect of wetting on pore texture and methane storage ability of NaOH activated anthracite // Fuel. 2007. V. 86. P. 287-293.
7. Jibril B.Y., Al-Maamari R.S., Hegde G., Al-Mandhary N., Houache O. Effects of feedstock pre-drying on carbonization of KOH-mixed bituminous coal in preparation of activated carbon // J. Anal. Appl. Pyrolysis. 2007. V. 80. P. 277-282.
8. Nowicki P., Pietrzak R., Wachowska H. Siberian anthracite as a precursor material for microporous activated carbons // Fuel. 2008. V. 87. P. 2037-2040.
9. Mikova N.M., Chesnokov N.V., Kuznetsov B.N. Study of High Porous Carbons Prepared by the Alkaline Activation of Anthracites // J. Siberian Federal University. Chemistry. 2009. V. 2. P. 3-10.
10. Durie R.A., Schafer H.N.S. The production of active carbon from brown coal in high yields // Fuel. 1979. V. 58 P. 472-476.
11. Guy P.J., Perry G.J. Victorian brown coal as a source of industrial carbons: a review // Fuel. 1992. V. 71. P. 1083-1086.
12. Guy P.J., Verheyen T.V., Heng S., Felber M.D., Perry G.J. Physical properties of activated carbons derived from alkali treated victorian brown coal / Proc. of Int. Conf. on Coal Science (23-27 October, 1989) Tokyo, Japan. V. 1. P. 21-24.

13. Amarasekera G., Scarlett M.J., Mainwaring D.E. Development of microporosity in carbons derived from alkali digested coal *Carbon*. 1998. V. 36. P. 1071-1078.
14. Schafer H.N.S. The production of active carbon from brown coal in high yields // *Fuel*. 1979. V. 58. P. 673-679.
15. Utz B.R., Nowak M.A., Fauth D.J. Nucleophilic properties of molten hydroxides in the desulfurization of coal and model compounds / *Proc. of Int. Conf. on Coal Science (23-27 October, 1989)*. Tokyo, Japan. V. 1. P. 197-200.
16. Steelink C. Electron paramagnetic resonance studies of humic acid and related model compounds // *Coal Science. Adv. Chem. Ser. 55 ACS*. Washington. 1966. P. 80-90.
17. Verheyen V., Rathbone R., Jagtoyen M., Derbyshire F. Activated extrudates by oxidation and KOH activation of bituminous coal // *Carbon*. 1995. V. 33. P. 763-772.
18. Rodae V.V., Golovin G.S., Papirova E.A. Composition of wax fraction of brown coal bitumen / *Proc. of the 8<sup>th</sup> Int. Conf. on Coal Science*. Amsterdam: Elsevier. – 1995. V. 1. P. 95-98.
19. Brunauer S., Emmett P.H., Teller E. Adsorption of gases in multimolecular layers // *J. Am. Chem. Soc.* 1938. V. 60. P. 309-319.
20. Barret E.P., Joyner L.C., Halenda P.P. The determination of pore volume and area distributions in porous substances. I. Computations from nitrogen isotherms // *J. Am. Chem. Soc.* 1951. V. 73. P. 373-380.
21. Dubinin M.M. Fundamentals of the theory of adsorption in micropores of carbon adsorbents: characteristics of their adsorption properties and microporous structures // *Carbon*. 1989. V. 27. P. 457-467.
22. Evans R., Marconi U.M.B., Tarazona P.J. Capillary condensation and adsorption in cylindrical and slit-like pores // *Chem. Soc. Faraday Trans.* 1986. V. II 82. P. 1763-1787.
23. Tamarkina Y.V., Maslova L.A., Khabarova T.V., Kucherenko V.A. Adsorption properties of carbon materials produced by thermolysis of brown coal in the presence of alkali metal hydroxides // *Russian Journal of Applied Chemistry*. 2008. V. 81. P. 1167-1170.
24. Kucherenko V.A., Shendrik T.G., Khabarova T.V., Tamarkina Yu.V. Influence of chemical activation temperature on forming porous structure of adsorbents from brown coal // *Journal of Siberian Federal University*. – 2009. – Vol. 2, is.3. – P. 223-231 (in Russian).
25. Xia K., Gao Q., Wu C., Song S., Ruan M. Activation, characterization and hydrogen storage properties of the nanoporous carbon from CMK-3 // *Carbon*. 2007. V. 45. P. 1989 – 1996.
26. Chmiola J., Yushin G., Gogotsi Y., Portet C., Simon P., Taberna P.L. Anomalous increase in carbon capacitance at pore sizes less than 1 nanometer // *Science*. 2006. V. 313. P. 1760-1763.
27. Lillo-Rodenas M.A., Cazorla-Amoros D., Linares-Solano A. Understanding chemical reactions between carbons and NaOH and KOH. An insight into the chemical activation mechanism // *Carbon*. 2003. V. 41. P. 267-275.
28. Yamashita Y., Ouchi K. Influence of alkali on the carbonization process // *Carbon*. 1982. V. 20. P. 47-53.
29. Clar E. *Polycyclic Hydrocarbons*. Academic Press: London 1964. – 391 p.

## **Конверсия александрийского бурого угля в микропористый углеродный материал в условиях щелочной активации**

**Ю.В. Тамаркина, Т.Г. Шендрик,  
В.А. Кучеренко, Т.В. Хабарова**

*Институт физико-органической химии и углехимии  
им. Л.М. Литвиненко НАН Украины,  
Украина 83114, Донецк, ул. Р. Люксембург, 70*

---

*Была изучена пористая структура активированного угля (АУ), полученного термоллизом бурого угля Александрийского месторождения (Украина), предварительно импрегнированного гидроксидом щелочного металла, МОН, где М = Li, Na, K. Было изучено, как меняются удельная поверхность, суммарный объем пор, объемы мезо- и микропор с изменением параметров процесса, таких как температура, соотношение щелочь/уголь (до 2 г/г) и природа катиона. Также было установлено распределение мезо- и микропор по размерам и влияние разных щелочей на развитие пористости. Очевидно, что микропористая система развивается при нагревании (от 400 °С до 800 °С) угля, импрегнированного КОН: удельная поверхность возрастает от 13 до 1005 м<sup>2</sup>/г, тогда как доля микропор увеличивается с 1 до 68 % общего объема пор. Микропористый материал формируется при 800 °С за 1 ч с выходом 30 %, удельной поверхностью 1005 м<sup>2</sup>/г, общим объемом пор 0,55 см<sup>3</sup>/г и объемом микропор 0,38 см<sup>3</sup>/г. Суммарный объем пор растет монотонно в ряду LiOH < NaOH < КОН.*

*Ключевые слова: бурый уголь, щелочная активация, микропористость.*

---